Cellular/Molecular

Critical Residues of the *Caenorhabditis elegans unc-2* Voltage-Gated Calcium Channel That Affect Behavioral and Physiological Properties

Eleanor A. Mathews,[1] Esperanza García,[1] Celia M. Santi,[1] Gregory P. Mullen,[2] Colin Thacker,[1] Donald G. Moerman,[2] and Terrance P. Snutch[1]

[1]Biotechnology Laboratory and [2]Department of Zoology, University of British Columbia, Vancouver, British Columbia, Canada V6T 1Z3

The *Caenorhabditis elegans unc-2* gene encodes a voltage-gated calcium channel α_1 subunit structurally related to mammalian dihydropyridine-insensitive high-threshold channels. In the present paper we describe the characterization of seven alleles of *unc-2*. Using an *unc-2* promoter-tagged green fluorescent protein construct, we show that *unc-2* is primarily expressed in motor neurons, several subsets of sensory neurons, and the HSN and VC neurons that control egg laying. Examination of behavioral phenotypes, including defecation, thrashing, and sensitivities to aldicarb and nicotine suggests that UNC-2 acts presynaptically to mediate both cholinergic and GABAergic neurotransmission. Sequence analysis of the *unc-2* alleles shows that *e55*, *ra605*, *ra606*, *ra609,* and *ra610* all are predicted to prematurely terminate and greatly reduce or eliminate *unc-2* function. In contrast, the *ra612* and *ra614* alleles are missense mutations resulting in the substitution of highly conserved residues in the C terminus and the domain IVS4-IVS5 linker, respectively. Heterologous expression of a rat brain P/Q-type channel containing the *ra612* mutation shows that the glycine to arginine substitution affects a variety of channel characteristics, including the voltage dependence of activation, steady-state inactivation, as well as channel kinetics. Overall, our findings suggest that UNC-2 plays a pivotal role in mediating a number of physiological processes in the nematode and also defines a number of critical residues important for calcium channel function *in vivo*.

Key words: **calcium channel; mutation; behavior; electrophysiology; presynaptic; *C. elegans***

Introduction

Voltage-gated calcium (Ca) channels play a central role in a number of biological processes, including neurotransmitter release, excitation–contraction coupling, regulation of gene expression, and neuronal migration. In addition, compounds that directly affect either Ca channels or proteins that modulate their activity are used to treat a number of cardiovascular and neurological pathologies (Miller, 2001). Understanding the nature of Ca channel functional diversity will provide insight into both normal calcium signaling mechanisms, as well as contributing to our understanding of the roles that these molecules play in various pathological conditions.

High-threshold Ca channels are multisubunit complexes consisting of four to five subunits designated α_1, $\alpha_2\delta$, β, and γ (for review, see Catterall, 2000). The α_1 subunit forms the voltage-sensor and channel proper, whereas the remaining proteins interact with the α_1 subunit to modulate channel activity. In mammals, five pharmacologically distinct types of Ca channels have been described (designated L-, N-, P/Q-, T-, and R-types) and that are encoded by 10 distinct α_1 subunit genes (Stea et al., 1995b; Catterall, 2000). Genetic and molecular studies have revealed the presence of three α_1 subunit genes in the nematode *Caenorhabditis elegans*: *unc-2* (Schafer and Kenyon, 1995), *egl-19* (Lee et al., 1997), and *cca-1* (for review, see Bargmann 1998) and which appear to be ancestral to the mammalian N/P/Q-, L-, and T- type channels, respectively. Genes encoding other Ca channel subunits have also been identified in the *C. elegans* genome: *unc-36* and T24F1.6 encode $\alpha_{2\delta}$ subunit homologues and *ccb-1* (T28F2.5) and W10C8.1 both encode putative β subunits (Bargmann, 1998).

Schafer and Kenyon (1995) first noted that the slow, uncoordinated movement and constitutive egg-laying defects displayed by *unc-2* mutants resembled the affects of adding exogenous serotonin to wild-type worms. In addition, unlike wild-type animals, *unc-2* worms were unable to adapt to either serotonin or dopamine (Schafer and Kenyon, 1995). Subsequently, it was shown that mutations in the *unc-36* gene exhibited similar mutant phenotypes to that of *unc-2,* suggesting that these two genes act together in a Ca- dependent pathway to modulate responses

Received Dec. 4, 2002; revised May 22, 2003; accepted May 22, 2003.

This work was supported by grants from the Canadian Institutes of Health Research (CIHR) of Canada to T.P.S. and D.G.M., fellowship support from the Human Frontiers Research Program to C.M.S., the British Columbia and Yukon Heart and Stroke Foundation to E.A.M., and a CIHR Senior Scientist Award to T.P.S. Some strains in this work were kindly provided by E. M. Jorgensen (University of Utah, Salt Lake City, UT), J. B. Rand (Oklahoma Medical Research Foundation, Oklahoma City, OK), and J. A. Hodgkin (University of Oxford, Oxford, UK). Additional strains were provided by the *Caenorhabditis* Genetics Center. We also thank A. Fire, G. Zamponi, and Y. Kohara for providing clones, J. Thomas for details pertaining to the defecation assay, B. Barstead for the λACT-RB2 cDNA library, and C. Bargmann for help with the identification of GFP fluorescent cells. Excellent technical assistance was provided by Tracy Evans and Daniel Malebranche.

Correspondence should be addressed to Terrance P. Snutch, Room 237–6174, University Boulevard, University of British Columbia, Vancouver, British Columbia, Canada V6T 1Z3. E-mail: snutch@zoology.ubc.ca.

E. A. Mathews' and G. P. Mullen's present address: Program in Molecular and Cellular Biology, Oklahoma Medical Research Foundation, Oklahoma City, OK 73104.

C. M. Santi's present address: Department of Anatomy and Neurobiology, Washington University School of Medicine, St. Louis, MO 63110.

E. García's present address: Centro de Investigaciones Biomedicas, Universidad de Colima, A.P. 199, Colima, 2800, Mexico.

 0270-6474/03/236537-09$15.00/0

to serotonin (Schafer and Kenyon, 1995; Schafer et al., 1996). Genetic mosaic analysis and *in situ* hybridization experiments have shown that UNC-2/UNC-36 both act in the HSN and/or VC neurons known to control egg laying in *C. elegans* (Schafer and Kenyon, 1995; Schafer et al., 1996). Mutations in *unc-2* have also been shown to affect migration of specific neuronal cells. For example, the sensory neuron AVM and the interneuron SDQR undergo aberrant postembryonic migrations in *unc-2* mutants (Tam et al., 2000). *unc-2* also plays an integral role in a Ca-dependent signal transduction pathway that controls the asymmetric expression of the *str-2* odorant receptor gene in the AWC sister sensory neurons (Troemel et al., 1999). In both processes, mutations in *unc-2* and *unc-36* show similar phenotypes, implying that these two gene products act in the same functional complex. Mutations in genes encoding factors that are known to regulate Ca channel α_1-subunits, such as CaM kinase II (*unc-43*) (Reiner et al., 1999; Rongo and Kaplan, 1999), syntaxin (*unc-64*) (Saifee et al., 1998), and G-proteins (*goa-1:* Lochrie et al., 1991; *gpb-1:* Brundage et al., 1996; Zwaal et al., 1996), have also been identified. Interestingly, genetic analysis of the Ca signaling pathways involving UNC-2 that affect cell migration and *str-2* odorant receptor gene expression have demonstrated that one of the downstream effectors is *unc-43*/CaM kinase II (Troemel et al., 1999; Tam et al., 2000). Taken together, these findings suggest that both potential modulators of Ca channel α_1-subunits and the α_1-subunits themselves function in a variety of complex physiological processes. Consequently, the coordinated analysis of these genes in *C. elegans* using genetic, behavioral, and electrophysiological methodologies should add to our understanding of Ca channel physiological functions *in vivo*.

Here we describe a comprehensive characterization of the *unc-2* gene and the isolation of six new alleles of *unc-2* as well as the canonical allele, *e55*. We also present evidence that *unc-2* acts as a presynaptic Ca channel to mediate both acetylcholine and GABA release in the nematode. Molecular analyses of the mutant *unc-2* alleles identifies highly conserved residues that contribute to Ca channel function *in vivo*. Introduction of the *ra612* allele into the mammalian P/Q-type channel shows that disruption of a conserved site in the C terminus dramatically affects channel voltage-dependent and kinetic properties.

Materials and Methods

Nematode strains and growth conditions. Nematodes were grown on nematode growth media (NGM) plates streaked with *Escherichia coli* (OP50 strain), as described (Brenner, 1974). Strains in this work include the wild-type strain N2; *unc-2(e55)*, CB55; *unc-2(ra605)* TS79, *unc-2(ra606)* TS80; *unc-2(ra609)* TS82; *unc-2(ra610)*, TS83; *unc-2(ra612)*, TS85; *unc-2(ra614)*, TS118; *unc-2(e55) dpy-3(e27)*, DM2601; *unc-25(e265)*, CB265; *unc-36(e251)*, CB251; *lin-15(n765)*; and *vaIs9*, TS67. The identification of the *ra605* and *ra610* mutations were previously reported in Tam et al. (2000).

Isolation of new unc-2 *alleles.* A non-complementation screen was used to isolate new alleles of *unc-2*. Briefly, N2 males were mutagenized with 50 mM ethyl methane sulfonate and crossed to *dpy-3(e27) unc-2(e55)* hermaphrodites. Twenty mating plates, each with six males and three hermaphrodites, were set up, and their progeny were screened for the presence of Unc non-Dpy progeny. Eleven independent Unc non-Dpy animals were identified and picked to new plates. From each plate, single Unc animals were transferred to new plates, and their progeny were scored for the presence of Dpy Uncs. Animals that failed to segregate Dpy Unc progeny were presumed to be homozygous for the new *unc-2* mutation. Strains were outcrossed at least three times before phenotypic analysis.

Phenotypic analyses of unc-2 *mutants.* Resistance of wild-type and mutant worms to aldicarb was performed as described (Miller et al., 1996). Briefly, 20 animals were placed on plates containing 0.5 mM aldicarb and assayed for paralysis at 10 min intervals for 3 hr. Animals, except for five individuals, were removed from the plates and then scored periodically over 1, 2, and 3 weeks for the production of viable progeny. To test for sensitivity to nicotine, plates were flooded with 1% nicotine solution.

To examine defects in movement, young adult hermaphrodites were transferred to a microtiter well containing 60 μl of M9 buffer. After a 2 min recovery period, thrashes were counted for 2 min (Miller et al., 1996). A thrash was defined as a change in direction of bending at the mid-body. Ten animals from each strain were examined. Defects in defecation were determined by examining young adult hermaphrodites with a dissecting microscope for the presence or absence of an expulsion event after each posterior body muscle contraction (pBoc) of the defecation cycle (Thomas, 1990; Miller et al., 1996). Ten animals from each strain were observed for 10 consecutive cycles.

cDNA cloning. Overlapping cDNAs encoding the *unc-2* gene were isolated from several sources. These included RT-PCR of total RNA prepared from a mixed population of worms and both PCR amplification and screening of a cDNA library (λACT-RB2; kindly provided by Robert Barstead, Oklahoma Medical Research Foundation, OK). The entire predicted *unc-2* open reading frame (ORF) is encoded by five overlapping cDNA clones, namely punc2.1, which included the putative initiator methionine codon; cDNA 82–43; cDNA10; cDNA1, and yk131b1 which contained the predicted *unc-2* poly(A) site (AATAAA) and the 3′ untranslated region (3′ UTR) (Fig. 1*A*). The cDNA clone yk131b1 was generously provided by Yuji Kohara (National Institute of Genetics, Japan). The composite sequence of the overlapping cDNA clones was submitted to GenBank (accession number AY264781). Existing GenBank entries for *unc-2* differ considerably from the sequence reported in this work. An explanation for this discrepancy is that previous GenBank submissions have been based on annotated predictions using the program GeneFinder rather than on actual physical comparison of cDNA and genomic sequences. Differences between the cDNA sequence described in this work and that from Tam et al. (2000) is attributable to the discovery of additional 5′ sequences and a nucleotide sequencing change in the 3′ end of the gene that altered the reading frame of the predicted gene product (see Results).

Identification of unc-2 *lesions.* To identify the nucleotide changes in the *unc-2* mutants, two approaches were used. The first involved the use of an RNase protection assay performed according to the procedure outlined in the Mismatch Detect II kit (Ambion). In the second approach genomic DNA encompassing the *unc-2* gene from the corresponding homozygous mutant animals was amplified, and the DNA sequence was determined directly.

unc-2::green fluorescent protein *fusion.* Long-range PCR was used to amplify the 5′ region of the *unc-2* gene and the predicted first three exons (Fig. 1*A*). Two fragments were amplified from genomic DNA. One included ~4 kb of 5′ sequence upstream from the first exon, along with a 6.8 kb region encompassing exons one and two. The second long-range PCR product was 4.1 kb in length, overlapping with the first product by 694 bp and ending within exon three. The second product was cloned into the vector pGEM-T easy. A green fluorescent protein (GFP) cassette isolated from the expression vector pPD95.70 (kindly provided by A. Fire) was then cloned in-frame with exon 3, generating the construct punc24.70. The 10.8 kb long-range PCR product was injected into the gonads of adult *lin-15(n765ts)* hermaphrodites along with punc24.70 and pJM23, which contains a wild-type copy of the *lin-15* gene. Transformants were rescued for the *lin-15* multivulval phenotype, and stable lines were established. The array from one of these lines was integrated, and GFP expression was examined in this strain, called TS67. Cell identification was based on the position and characteristic morphology of GFP-positive cell nuclei using fluorescence and Nomarski differential interference microscopy.

Construction of rat brain α_{1A} mutant. unc-2 mutations corresponding to *e55* and *ra612* were introduced into the rat brain α_{1A}/Ca_v2.1 cDNA by site-directed mutagenesis. Details of the procedures used can be obtained from the authors on request. All mutations were made in the rat α_{1A}/Ca_v2.1 clone pc3RBA1 (Starr et al., 1991). To generate the corresponding *e55* mutation the α_{1A}/Ca_v2.1 cDNA was truncated by the introduction of a stop codon after the R477 codon. The construct pα_{1A}55 encodes only the N terminus of the rat α_{1A}/Ca_v2.1 subunit ending in the domain I-II

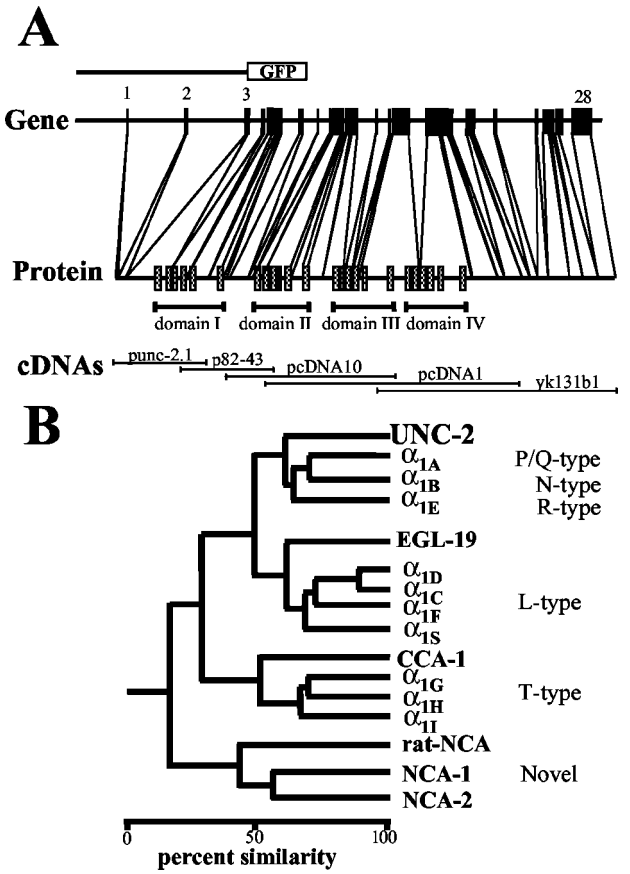

Figure 1. *unc-2* gene structure and phylogenetic comparison. *A,* Organization of the *unc-2* gene structure. Shown is the intron–exon structure of the *unc-2* gene (Gene), including the genomic region used to generate the *unc-2*::GFP fusion construct (top). Also shown are the regions of the predicted gene product (Protein) that are encoded by the corresponding exons and the overlapping cDNAs or RT-PCT products used to determine the gene structure (cDNAs). *B,* Phylogenetic comparison of UNC-2 with other *C. elegans* and mammalian Ca channel α_1 subunits. The predicted amino acid sequences of representatives of each class of Ca channel α_1 subunit and the novel NCA ion channel family α_1 subunits were compared pairwise, and the percentage similarities were plotted. GenBank accession numbers for the Ca channels: rat α_{1A}/Ca_v2.1, M64373; rat α_{1B}/Ca_v2.2, M92905; rat α_{1C}/Ca_v1.2, M67515; rat α_{1E}/Ca_v2.3, L15453; human α_{1F}/Ca_v1.4, AJ224874; rabbit α_{1S}/Ca_v1.1, M23919; rat α_{1D}/Ca_v1.3, (E. Mathews and T. Snutch, unpublished results); UNC-2, AY264781 (this work); EGL-19, AF023602; CCA-1, (AY313898); rat brain NCA, AAC68885.1; and *C. elegans* NCA-1 and NCA-2 α_1 subunits (cosmids C11D2.6 and C27F2.5; and K. Hamming and T. P. Snutch, unpublished results).

linker. Plasmid pmα_{1A}-612 contains the corresponding *ra612* mutation in which the G1817 codon (GGC) was changed to arginine (CGT).

Electrophysiology and data analysis. Human embryonic kidney (HEK)-tsa201 cells were transiently transfected by the Ca phosphate precipitation method with an equimolar ratio of cDNAs encoding either the wild-type rat brain Ca channel α_{1A}/Ca_V2.1 or one of the plasmids carrying the engineered mutation plus the rat brain β1b and α2δ ancillary subunits. Coexpression of CD8 antigen was used to visually identify cells for electrophysiological experiments through the binding of anti-CD8 antibody-coated microspheres (Dynal, Great Neck, NY). Whole-cell inward currents were recorded 24–48 hr after transfection with an Axopatch 200B patch-clamp amplifier (Axon Instruments, Foster City, CA). Recordings were filtered at 2 kHz and acquired using pClamp software, version 6.03 (Axon Instruments). The extracellular recording solution contained either 5 mM $BaCl_2$ or 5 mM $CaCl_2$ and 1 mM $MgCl_2$, 10 mM HEPES, 40 mM TEACl, 10 mM glucose, and 87.5 mM CsCl, pH 7.4. Pipettes of typical resistances ranging from 2 to 4 MΩ were filled with internal solution containing (in mM): 105 CsCl, 25 TEACl, 1 $CaCl_2$, 11 EGTA, and 10 HEPES, pH 7.2. The voltage dependence of activation was analyzed by step depolarizations from a holding potential of −120 mV to various test potentials ranging from −60 to +30 mV. Normalized current amplitudes were plotted as a function of membrane potential, and *I–V* curves were fitted according to equation: $I = \{G_{max}(V_m - V_{rev})\}/\{1 + \exp[(V_m - V_{0.5})/k_a]\}$, where G is membrane conductance, V_{rev} is the reversal potential, $V_{0.5}$ is the midpoint, and k_a the slope of the voltage dependence. To measure steady-state inactivation profiles, conditioning prepulses (15 sec) from −120 to 40 mV in 10 mV steps were applied, and the membrane was then stepped to the peak of the *I–V* curve. Currents were normalized to the maximal value obtained at the test pulse and plotted as a function of the prepulse potential. Data were fitted with Boltzmann equations ($I/I_{max} = \{1 + \exp[(V - V_{0.5})/k_i]\} - 1$). All experiments were performed at room temperature. Recordings were analyzed using Clampfit 6.03 (Axon Instruments); figures and nonlinear regressions were done using the Origin software (version 6.0; Microcal, Northampton, MA). Data are presented as mean ± SEM. Significant differences were determined using Student's *t* test with the significance value set at $p < 0.01$.

Results

Isolation and characterization of the *unc-2* gene

Previous analysis of the *unc-2* gene suggested that it encoded the α_1 subunit of a non-L-type high voltage-activated (HVA) Ca channel (Schafer and Kenyon, 1995). To characterize the complete *unc-2* gene structure and predicted coding region, a combination of cDNA cloning and RT-PCR were used. Comparison of the cDNA and nematode genomic sequences show that the *unc-2* gene consists of at least 28 exons and 27 introns encompassing a region of ~25 kb (Fig. 1*A*). The exons range in size from 47 to 879 bp. Exon one contains the putative ATG initiation methionine, and exon 28 (determined through cDNA sequence analysis) contains an in frame termination codon (TAG) and a potential polyadenylation sequence (AATAAA) located 688 bp downstream. The majority of introns within *unc-2* are between 40 and 60 bp, although introns one and two are 5.4 and 4.9 kb, respectively. With the exception of intron eight, all introns conform to the GU-AG splice site consensus sequence. Intron eight starts with a GC dinucleotide, which has been previously noted, albeit rarely, at 5′ splice sites in *C. elegans* (for review, see Blumenthal and Steward, 1997).

Compared with the previously reported primary sequence for *unc-2* (Schafer and Kenyon, 1995; Tam et al., 2000), we found an additional 161 nucleotides in the 5′ coding and non-coding regions and that resulted in 42 additional amino acids, including the putative initiator methionine. In the 3′ coding region, we also found that an additional nucleotide insertion caused a frame shift and resulted in replacement of the C terminal 53 residues by 335 new amino acids (GenBank accession number AY264781). Overall, the longest open reading frame of *unc-2* encodes a 2027 amino acid polypeptide with a predicted molecular weight of 231 kDa (Figs. 1*A*, 2). UNC-2 has features common to all voltage-gated Ca channels, including four homologous domains (I-IV) each containing six hydrophobic membrane-spanning segments (S1–S6), which share significant sequence similarity with the analogous regions of other Ca channels. In addition, UNC-2 possesses other features that are well conserved among vertebrate high voltage-activated Ca channels, including a G$\beta\gamma$ (De Waard et al., 1997; Zamponi et al., 1997) and Ca channel β subunit binding motifs (Pragnell et al., 1994) in the domain I linker, EF-hand (Babitch, 1990) and IQ motifs (Lee et al., 1999; DeMaria et al., 2001) in the C terminus distal to domain IV, and four conserved glutamate residues in the P-loops that confer Ca^{2+} selectivity (Heinemann et al., 1992; Yang et al., 1993).

Comparatively, UNC-2 is more closely related to the mammalian DHP-insensitive α_1 subunit classes (rat brain α_{1B} = 73% similarity; α_{1A} = 67%; α_{1E} = 66%) than to the L-type channels (~55% similarity) (Fig. 1*b*). A defining feature of L-type channels is their sensitivities to DHPs and phenyalkylamines and the

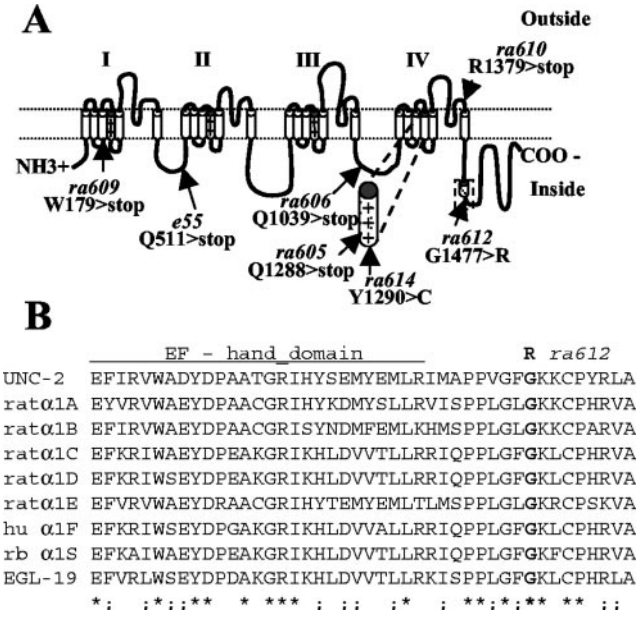

Figure 2. Schematic representation of the location of molecular lesions within *UNC-2*. *A,* The major structural domains including the four domains (I–IV), the EF-hand domain in the C terminal region, and the locations of identified mutations are indicated. *B,* Alignment of the UNC-2 sequence within the boxed area indicated in *A* with the corresponding region of the mammalian and *C. elegans* EGL-19 L-type Ca channel α_1 subunits. Identical residues (*), conserved residues (:). The C terminal region shown encompasses the conserved EF-hand domain (single overlined). Note that the *unc-2*(*ra612*) mutation changes a conserved glycine residue (bold), which resides between the EF-hand and an IQ-like motif further downstream.

specific amino acids of the L-type channels required to interact with these agents have been described (Moreno, 1999). Of the four specific residues in domain IV identified to confer DHP and phenyalkylamine binding in the L-type channels (Tang et al., 1993; Grabner et al., 1996; Schuster et al., 1996), UNC-2 does not match exactly at any position but instead possesses residues identical to those found only in the non-DHP-sensitive high voltage-activated Ca channel subfamily.

Isolation and characterization of novel *unc-2* mutations

Using a non-complementation screen, six new EMS-induced alleles of *unc-2* were isolated from ~20,000 F1 progeny examined. All alleles showed locomotor defects typical for *unc-2* mutants, as described previously (Schafer and Kenyon, 1995; Schafer et al., 1996). However, differences in the mobility of mutant animals were noted. For example, the canonical *unc-2* allele, *e55*, showed a severe movement deficit, as did *ra605, ra606*, *ra609,* and *ra610.* In contrast, the *ra612* and *ra614* alleles showed moderate to mild defects in movement. To understand the underlying differences between the mutants, the molecular lesions of several *unc-2* alleles were determined (see Materials and Methods). The results show that five mutations, *e55*, *ra605*, *ra606*, *ra609,* and *ra610* are all single base substitutions predicted to result in premature stop codons and, hence, truncated proteins (Fig. 2*A*). The *e55* allele is a change of glutamine 511 to a stop in the domain I-II linker, the *ra605* allele a change of glutamine 1288 to stop in domain IV S4, *ra606* a change of glutamine 1039 to a stop in the domain III-IV loop, *ra609* a change of tryptophan 179 to a stop in the IS3 transmembrane domain, and *ra610* a change of arginine 1379 to stop in domain IV S5-S6. All of these mutations result in a severe uncoordinated phenotype, and together with their identification as premature stop codons in highly conserved structural regions of the channel are therefore likely to represent the *unc-2* null phenotype (see below).

Two alleles, *ra612* and *ra614*, were found to be missense mutations. The *ra612* mutation altered glycine 1477 to an arginine in the C terminus in a region flanked by a conserved EF-hand and a downstream-IQ domain (Fig. 2*B*). The *ra614* allele was found to possess an A to G mutation that alters a conserved tyrosine 1255 to a cysteine in the domain IVS4-IVS5 linker. Interestingly, the residues altered in both mutants are conserved in all vertebrate high voltage-activated Ca channels cloned to date including all splice variants of $\alpha_{1A}/Ca_v2.1$ and $\alpha_{1B}/Ca_v2.2$ (Stea et al., 1995b).

Phenotypic analysis of *unc-2* alleles

In an attempt to further correlate the various *unc-2* molecular lesions with locomotor activity, several phenotypic analyses were performed. Initially, *e55*, *ra605*, *ra609,* and *ra612* were examined for their sensitivities to aldicarb and nicotine. *unc-2* mutants have previously been shown to be resistant to the effects of the AChE inhibitor aldicarb, implicating the UNC-2 protein in cholinergic transmission (Miller et al., 1996). Within 1 hr of being placed on NGM plates containing 0.5 mM aldicarb, wild-type animals became paralyzed, and the body wall muscles hypercontracted, causing eggs to be extruded from the uterus. In contrast, animals for the four *unc-2* alleles tested were not noticeably affected after 1 hr of exposure (Fig. 3*A*). After 1 week of aldicarb exposure, the wild-type animals had died without successfully reproducing. Again, in contrast to wild-type animals, the four *unc-2* strains examined were hypercontracted by this point, but the original animals plated remained alive, and living progeny were also present. Differences among the four *unc-2* alleles tested became apparent after 3 weeks of aldicarb exposure. Whereas all four strains produced some viable progeny, there were ~33–50% more animals on the *e55*, *ra605,* and *ra609* plates than on the *ra612* plates (Fig. 3*B*).

The addition of the acetylcholine agonist nicotine to *C. elegans* stimulates postsynaptic acetylcholine receptors causing contraction of the body wall muscles. Treatment of wild-type and the four *unc-2* strains with nicotine caused both wild-type and mutant animals to hypercontract (data not shown). Because nicotine acts postsynaptically, these results suggest that mutations in *unc-2* do not directly affect the postsynaptic transmission machinery. Taken together with the effects of aldicarb, the data also suggest that mutations in *unc-2* most likely reduce ACh release at the neuromuscular junction, consistent with a role for UNC-2 as a presynaptic Ca channel that contributes to triggering neurotransmitter release.

For a more quantitative assessment of the neurotransmission defects in *unc-2*, we focused on the behaviors of locomotion and defecation. These behaviors are chiefly mediated by two different neurotransmitters, ACh and GABA (for review, see Rand and Nonet, 1997). As previously noted, *unc-2* mutants are slow moving and resistant to the AChE inhibitor aldicarb, suggesting that cholinergic transmission is impaired (Miller et al., 1996). Using a thrashing assay in liquid media, we quantified the extent of the impairment in various *unc-2* alleles. Thrashing was significantly reduced in *e55, ra605*, *ra609,* and *ra612* mutants compared with wild-type animals. Figure 3*C* shows that thrashing of *e55, ra605,* and *ra609* mutants was reduced to <3% of wild-type rates measured under similar conditions. Thrashing in *ra612* mutants was reduced to 6.5% of thrashing rates compared with wild-type, a value that is significantly different from both wild-type animals and the *unc-2* mutants examined (Fig. 3*C*).

The results of the thrashing assay provide further support for a defect in cholinergic transmission in *unc-2* animals. To assess the effects of mutations in *unc-2* on the release of another neuro-

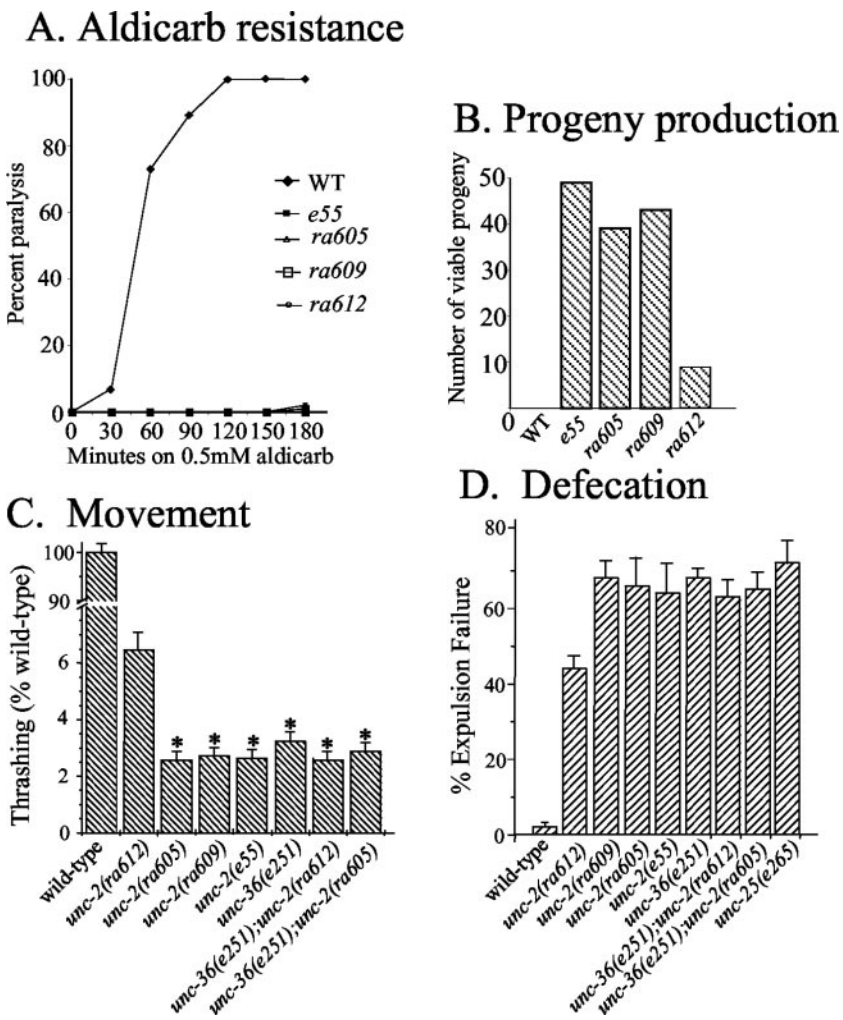

Figure 3. Behavioral analysis of *unc-2* mutants. *A*, *B*, *unc-2* mutants are resistant to the ACh esterase inhibitor aldicarb. Incubation of wild-type worms (filled diamonds) on 0.5 mM aldicarb (*A*) resulted in complete paralysis within ~120 min. In contrast, the *unc-2* mutants *e55*, *ra605*, *ra609*, and *ra612* showed resistance to aldicarb over the 3 hr period of observation. *B*, Continued growth of wild-type worms on aldicarb resulted in both a failure to survive and to produce progeny. The various *unc-2* mutants were able to survive continued growth on aldicarb for at least 3 weeks, even though the animals became hypercontracted. In addition, viable progeny were produced by the *unc-2* mutants, although differences in the number of progeny were observed. The nonsense mutants *e55*, *ra605*, and *ra609* segregated more progeny than the *ra612* mutant, suggesting that ACh release and, hence, viability was more impaired by aldicarb for the *ra612* animals. *C*, Thrashing assays were performed to characterize the affect of the *unc-2* lesions on worm body movement in fluid (for a definition of thrashing see Materials and Methods). Thrashing was reduced in *ra612* animals as compared with wild-type but was significantly less severe than that displayed by alleles *e55*, *ra605*, and *ra609*, the *unc-36* mutant, and the *unc-36*;*unc-2*(*ra612*) double mutant. *D*, Defects in defecation were scored as failure of EMCs during the defecation process. The percentage of failure of EMCs was compared with that of wild-type and the severe defecation mutant *unc-25*. *ra612* animals, although deficient in EMCs, were significantly less severe than *e55*, *ra605*, *ra609*, *unc-36*, and *unc-25* mutant animals. As predicted, the *unc-36*; *unc-2*(*ra612*) double mutant shows a defecation defect comparable with *unc-36* and severe *unc-2* alleles.

transmitter, we examined the expulsion step of the defecation process [enteric muscle contraction (EMC)]. EMC is mediated by GABA, and failure of EMC is indicative of a defect in GABA neurotransmission (McIntire et al., 1993a,b). As shown in Figure 3*D*, the expulsion failure rates of the *unc-2* mutants were significantly different from that of wild-type. Wild-type animals failed to defecate in <2% of cycles, whereas *ra612* mutants had an ~44% failure rate, and *e55*, *ra605*, and *ra609* animals failed ~70% of the time. Interestingly, the failure rates of the latter *unc-2* mutants were similar to those of *unc-25(e265)* animals, which are completely defective in GABA biosynthesis (Jin et al., 1999). Overall, the data are consistent with the notion that UNC-2 functions presynaptically to affect the release of the neurotransmitters ACh and GABA.

The *unc-36* gene encodes a homolog of the mammalian Ca channel $\alpha_2\delta$ subunit, and genetic analyses suggest that *unc-2* and *unc-36* may function as part of the same protein complex *in vivo* (Schafer and Ken-yon, 1995; Schafer et al., 1996). A prediction of this hypothesis is that *unc-36(null)*; *unc-2(null)* double mutants should have no worse a phenotype than either single mutant alone. In addition, it would be expected that *unc-36*; *unc-2(ra612)* double mutants should be more severe than *unc-2(ra612)* single mutants, but no worse than either *unc-36* or *unc-2* null mutants. To test this notion we constructed *unc-36(e251)*; *unc-2(ra605)*, and *unc-36(e251); unc-2(ra612)* double mutants. In all cases, the double mutants were indistinguishable from either the *unc-36(e251)* or *unc-2(ra605)* single mutants in their thrashing and defecation behaviors (Fig. 3*C*,*D*). Taken together, the data are consistent with the hypothesis that UNC-36 and UNC-2 function as part of the same Ca channel complex *in vivo*.

unc-2 gene expression pattern

The results of the behavioral studies suggested that UNC-2 functions primarily in the nervous system and plays a prominent role in synaptic release. To confirm this hypothesis, we constructed an *unc-2*::GFP reporter construct to determine the expression pattern of the *unc-2* gene in transformed animals. GFP fluorescence was found to be primarily localized within the nervous system (Fig. 4). Expression was first observed late in embryogenesis at ~450 min of development when most neurons have been generated, and continued throughout development to the adult stage. Of particular note, in contrast to previously reported *in situ* hybridization results (Schafer and Kenyon, 1995), GFP expression was observed only a subset of pharyngeal muscle cells but not in other types of muscle tissues.

The *unc-2* reporter gene was expressed in most motor neurons in the ventral nerve cord, nerve ring motoneurons—interneurons, and the touch cells (Fig. 4*A*). Postembryonic cell migration of the touch cell AVM and its sister, the interneuron SDQR, are often perturbed in *unc-2* mutant animals (Tam et al., 2000). Examination of the *unc-2::GFP* transgenic animals showed expression of the reporter gene in these two cells (Fig. 4*B*), suggesting that UNC-2 activity is required within AVM and SDQR to control their migration. A number of neurons in the head and tail regions were also observed to express the *unc-2::GFP* reporter gene. Of particular note, neurons identified in the head included the olfactory sensory cells AWC (Fig. 4*C*). UNC-2 has been shown to function in a Ca-dependent pathway that controls the asymmetric expression of the *str-2* olfactory receptor gene be-

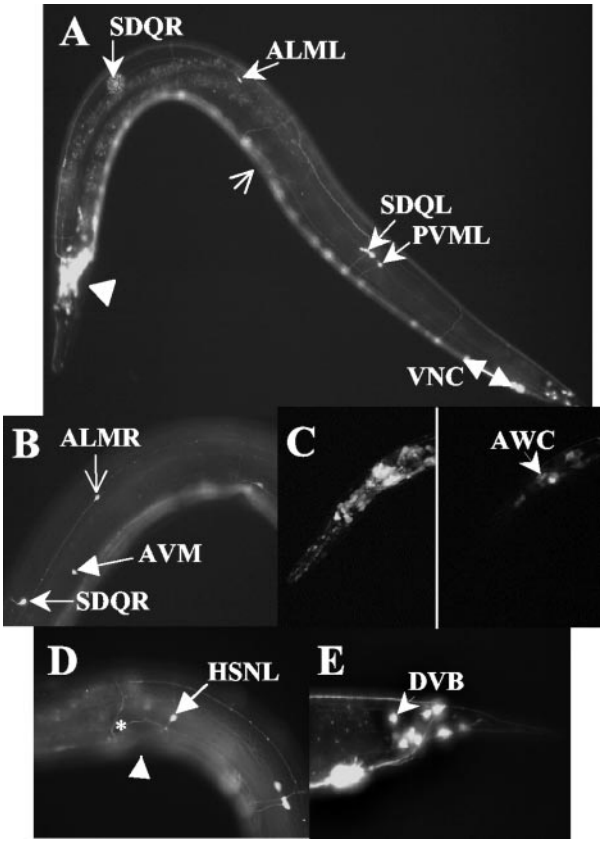

Figure 4. Expression of an *unc-2::GFP* fusion construct in transgenic animals. *A,* GFP fluorescence exhibited by a typical transgenic L3 larva (left side view of animal). Expression is observed in most sensory neurons in the head (filled arrowhead), as well as a subset of motor neurons in the ventral nerve cord (VNC, double arrowhead). Expression of the GFP reporter is also observed in the interneurons SDQL and SDQR (not in focus) and the touch receptors including ALM and PVM. *B,* Right side view showing expression in the SDQR interneuron and the touch cells AVM and ALM. *C,* Confocal images of the head region of an L1 larva. The left image is a composite confocal z-series of the entire head showing all GFP fluorescent cells, whereas the single slice on right shows expression of the reporter construct in a single AWC sensory neuron cell body. Expression of *unc-2::GFP* was observed in both sister AWC cells, although for clarity only one side of the head is shown. *D,* Expression of *unc-2::GFP* in the HSN (arrow) and VC neurons that control egg-laying. The cell bodies of the VC neurons are located in the ventral nerve cord and are not in the same focal plane. Processes extending from the more anterior VCs that innervate the vulval muscles are indicated by the star (*). *E,* Expression of *unc-2::GFP* in the pre-anal, dorsal-rectal, and lumbar ganglia of the tail. GFP fluorescence in the DVB neuron (arrowhead) which is required for defecation is indicated. The barbed arrow in *A* and the triangle in *D* represent the position of the vulva. In all panels, the anterior of the animals is positioned to the left, and the dorsal side is topmost.

tween the two sister AWC cells that reside on opposite sides of the animal. GFP expression was also observed in both the HSN and VC neurons (Fig. 4*D*) which together control egg laying in the hermaphrodite and support a previously proposed role for UNC-2 in this process. Cells expressing GFP in the tail region included the GABAergic neuron DVB (Fig. 4*E*), which together with AVL controls the enteric muscle contractions required for proper defecation (McIntire et al., 1993b). The impaired expression of UNC-2 in DVB may explain the defecation defects exhibited by the *unc-2* mutants.

Biophysical consequences of the *e55* and *ra612* mutations

As described above, the *e55*, *ra605*, *ra606*, *ra609,* and *ra610* alleles would all result in premature truncation of the *unc-2* gene product and thus would be predicted to result in no channel function. Of particular interest among these nonsense alleles, the *e55* premature stop mutation resides in the I-II loop and might allow expression of a single domain truncated product that could lead to the formation of functional voltage-gated channels with a structure similar to that for certain types of single domain voltage-gated potassium channels. To test this possibility, the corresponding *e55* mutation (R477stop) was introduced into the rat brain α_{1A}/Ca_v2.1 (P/Q-type) cDNA and transfected into HEKtsa201 cells (together with rat brain β1b and α2δ subunits). As shown in Figure 5*A*, cells transfected with the plasmid did not result in detectable currents using conditions identical to that for cells transfected with wild-type rat brain α_{1A}/Ca_v2.1 cDNA. These results, together with the genetic analysis of *e55*, suggest that the nonsense mutation fails to produce functional voltage-gated Ca channels.

Of the three missense mutations examined, the *ra612* allele with a lesion in the conserved C terminal domain, appeared to be the most interesting to pursue regarding functional analyses. The glycine residue at position 1477 is conserved among all high voltage-activated Ca channels and is located within a region flanked by an upstream Ca-binding EF-hand motif and a downstream IQ calmodulin binding motif. To test the effect of the G1477R mutation on channel physiological properties, we introduced the corresponding change (G1817R) into the α_{1A} P/Q-type channel and expressed the resulting construct in HEKtsa201 cells.

Currents recorded from HEK cells expressing wild-type α_{1A}/Ca_v2.1 (Fig. 5*B*) inactivated slowly during a test pulse to 0 mV ($\tau_{inact} = \sim$200 msec; $n = 5$). In contrast, $\alpha_{1A\text{-}612}$ currents decayed rapidly, with a biexponential time course ($\tau_1 = 14$ msec, $\tau_2 = 50$ msec; $n = 5$). At the end of a 200 msec test pulse, wild-type and mutant currents had decayed to 43 ± 4% ($n = 5$) and 94 ± 1% ($n = 5$) of the peak current, respectively. Comparison of the extent of inactivation measured as the magnitude of residual current as a function of membrane potential showed that the degree of inactivation of $\alpha_{1A\text{-}612}$ decreased monotonically with depolarization and reached a plateau at ~20% of the maximum current.

The current–voltage relationship for the $\alpha_{1A\text{-}612}$ channel was shifted ~10 mV more positive than that of the wild-type channel (Fig. 5*C*). In 5 mM Ba, currents through the wild-type α_{1A}/Ca_v2.1 channels first activated at approximately −30 mV and peaked at approximately −10 mV. In contrast, $\alpha_{1A\text{-}612}$ channels activated and peaked after depolarizations to −20 and 0 mV, respectively. No significant differences were detected in the voltage dependence of activation ($K_a\,\alpha_{1A} = 3.97 \pm 1.1$, $n = 5$; $K_a\,\alpha_{1A\text{-}612} = 4.03 \pm 1.2$; $n = 13$).

Comparison of the steady-state inactivation properties of the wild-type α_{1A}/Ca_v2.1 and $\alpha_{1A\text{-}612}$ mutant channels demonstrated significant differences in the potential at which half of the current was inactivated ($V_{0.5[inact]}$) (Fig. 5*D*). Compared with α_{1A}/Ca_v2.1, the voltage dependence of inactivation of $\alpha_{1A\text{-}612}$ was shifted by ~20 mV to more hyperpolarized potentials ($V_{0.5[inact]}$ for: α_{1A}/Ca_v2.1 = −52.5 ± 0.2 mV, $n = 4$; $\alpha_{1A\text{-}612}$ = -73.6 ± 0.4 mV, $n = 6$). Figure 5*E* shows that the current densities for the wild-type mutant *ra612* mutant channels were comparable using either Ba or Ca as the charge carriers ($n = 13$, wild-type in Ca; $n = 11$, mutant in Ca; $n = 8$, wild-type in Ba; $n = 13$, mutant in Ba). The fraction of noninactivating current was not affected by using Ca as the charge carrier, and kinetics of inactivation did not depend on the nature of the permeant ion (Fig. 6), suggesting that the inactivation mechanism produced by the G1447R mutation is unlikely caused by to alteration of a typical Ca-dependent process.

Discussion

Structural characterization of *unc-2*

The initial description of the *unc-2* gene structure and predicted UNC-2 protein were derived from the partial sequence from the nematode genome-sequencing project (Schafer and Kenyon,

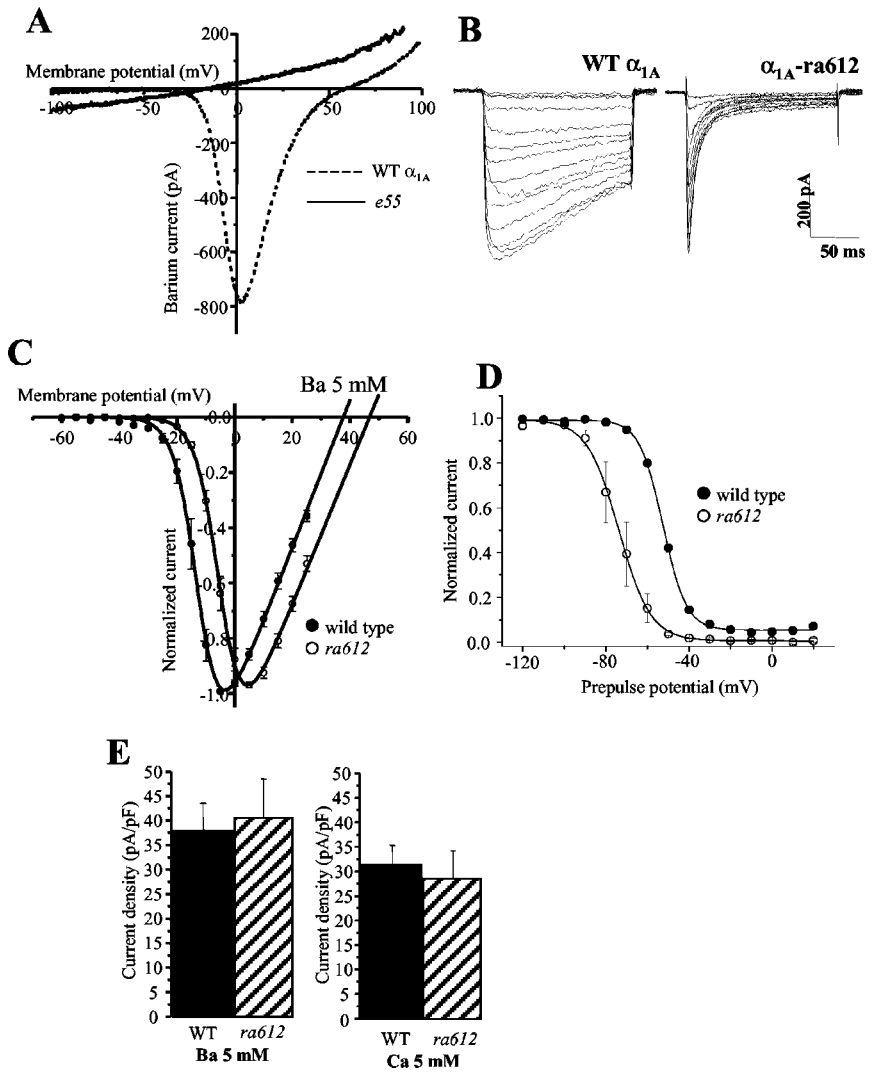

Figure 5. Functional consequences of the *e55* and *ra612* mutations on properties of the rat brain P/Q-type channel. *A,* Transfection of a rat α_{1A} cDNA containing the corresponding *e55* nonsense mutation failed to produce any currents (solid line) compared with those obtained from wild-type α_{1A} cDNA (dashed line). *B,* Representative traces of barium currents obtained from HEK cells transfected with either wild-type rat brain α_{1A} or $\alpha_{1A\text{-}612}$. Currents were evoked by stepping membrane potential for 200 msec to voltages between −60 and 25 mV in 5 mV increments from a $V_h = -120$ mV. The *ra612* missense mutation (G1477R) at the proximal region of the α_{1A} C tail modifies the kinetics of macroscopic inactivation of inward currents recorded in 5 mM external barium. *C, ra612* shifts the voltage dependence of channel activation to more depolarized potentials. Normalized peak current amplitude was plotted as a function of membrane potential to obtain the *I–V* relationship. Values obtained from the best fits of data (smooth curves) are: wild-type α_{1A} $V_{0.5} = -12.27 \pm 0.17$ mV, $k = 3.97 \pm 0.11$ mV ($n = 5$), $\alpha_{1A\text{-}612}$ $V_{0.5} = -4.64 \pm 0.22$ mV, $k = 4.03 \pm 0.12$ mV ($n = 13$). *D, ra612* causes a negative shift in the steady-state inactivation curves. Smooth-curve fits to data corresponding to α_{1A} (filled circles) and $\alpha_{1A\text{-}612}$ (hollow circles) showed a shift in the midpoint voltage and the slope factor (k_i) for steady-state inactivation: $\alpha_{1A\text{-}612}$ $V_{0.5} = -73.64 \pm 0.37$ mV, $K_i = 7.6 \pm 0.3$ mV ($n = 6$). α_{1A} $V_{0.5} = -52.47 \pm 0.18$ mV, $K_i = 5.6 \pm 0.1$ mV ($n = 4$). Note that the error bars for the wild-type α_{1A} channel are smaller than the symbol size. *E,* Current densities for wild-type and *ra612* mutant channels showed no significant difference when measured using either Ba or Ca as the charge carrier ($n = 13$, wild-type in Ca; $n = 11$, mutant in Ca; $n = 8$, wild-type in Ba; $n = 13$, mutant in Ba). All α_1 subunits constructs were coexpressed with rat brain β1b and $\alpha_2\delta$ subunits. Data are presented as mean ± SEM. Significant differences were determined using Student's *t* test with the significance value set at $p < 0.01$.

1995). The present study extends the initial *unc-2* gene characterization and provides a more complete and detailed understanding of the intron/exon boundaries and the UNC-2 protein. The first two introns of *unc-2* are quite large, spanning 5.4 and 4.9 kb, respectively. Although introns in *C. elegans* are mostly <60 bp in size, a number of genes contain large introns near their 5′ ends. In some cases, these large introns have been shown to contain regulatory elements such as alternative promoters or transcriptional enhancers (Blumenthal and Steward, 1997). There does not appear to be any obvious relationship between the intron/exon structure of the *unc-2* gene and the structural domains of the UNC-2 protein. For example, the putative transmembrane regions of domain I are encoded by five exons with no distinct boundaries that define any particular transmembrane region. By comparison, the majority of domain IV is encoded by only two exons. Furthermore, some exons encode portions of adjacent domains, such as with exon 17 that contains the last two transmembrane segments from domain III as well as the first two transmembrane segments of domain IV.

The predicted UNC-2 protein is structurally similar to other HVA Ca channel α_1 subunits and is most closely related to the DHP-insensitive α_1 subunit classes (N- and P/Q-type channels). Although the overall structure of UNC-2 is well conserved with its mammalian counterparts, the predicted intracellular domain II–III loop is considerably shorter and consists of only 97 residues, as compared with the ~500 residues encoded by the mammalian α_{1A} P/Q-type and α_{1B} N-type subunits. In this respect, UNC-2 is more similar in structure to the mammalian L-type and the *Drosophila* Dmca1A α_1 subunits. In the mammalian P/Q-type and N-type channel domain II-III linkers, the Synprint site has shown to be required for the physical interaction of SNARE proteins involved in eliciting presynaptic neurotransmitter release (Sheng et al., 1994, 1996; Rettig et al., 1996, 1997). The physical binding of the SNARE protein syntaxin to the Synprint site results in modulation of channel steady-state inactivation properties (Bezprozvanny et al., 1995) and also a negative feedback between Ca channel function and Ca-dependent gene regulation (Sutton et al., 1999). The lack of a readily identifiable Synprint site in UNC-2 suggests that the mechanisms of neurotransmitter release and the control of Ca channel regulation in *C. elegans* may differ from those in vertebrates.

UNC-2 contributes to both cholinergic and GABAergic neurotransmission

The *unc-2* mutant phenotype is primarily similar to that of mutants known to be defective in neurotransmission (Rand and Nonet, 1997). Furthermore, *unc-2* animals are aldicarb-resistant (Miller et al., 1996), implicating UNC-2 specifically in cholinergic neurotransmission. The wild-type response of *unc-2* animals to levamisole (Miller et al., 1996) and nicotine indicates that the aldicarb resistance is not caused by an abnormal response to ACh by the postsynaptic cell. Furthermore, expression of an *unc-2* promoter::GFP fusion revealed fluorescence in the nervous system, but not the body wall, uterine, or vulval musculature. These

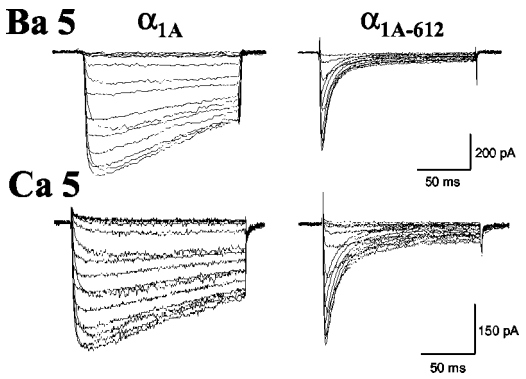

Figure 6. Fast decay of ion currents through $\alpha_{1A\text{-}612}$ channels is not dependent on the charge carrier. Currents recorded from HEK cells expressing wild-type α_{1A} or $\alpha_{1A\text{-}612}$ in either 5 mM Ba (top) or 5 mM Ca (bottom). Inward currents were elicited by 190 msec step depolarizations between −60 and 35 mV in 5 mV increments from a holding potential of −120 mV. Note the absence of calcium-dependent inactivation. Scale bars are the same for wild-type and mutant channels on each panel.

observations suggest that UNC-2 primarily functions in the nervous system to regulate neurotransmitter release.

In addition to aberrant locomotor behavior, *unc-2* mutants are defective in EMC of the defecation motor program (Miller et al., 1996). The AVL and DVB neurons that stimulate the contraction of the enteric muscles are GABAergic. Thus, the *unc-2* gene product appears to play a role in the release of GABA as well as ACh and may have a generalized role in neurotransmission in *C. elegans.*

The observed behavioral, pharmacological, and cellular expression studies suggest that UNC-2 functions in neurons in *C. elegans* in a manner analogous to that of the presynaptic N- and P/Q-type channels in vertebrate CNS. Null mutations in *cha-1* and *unc-17*, which encode choline acetyltransferase and a synaptic vesicle ACh transporter, respectively, completely abrogate ACh release. These mutants are not viable, arresting at the L1 stage of development (Nonet et al., 1993). In contrast, the *unc-2* null phenotype predicted by mutants *e55*, *ra605*, *ra606*, *ra609,* and *ra610* are all significantly milder than that of *cha-1* and *unc-17*, suggesting that even in the absence of *unc-2*, there is some residual release of ACh from motor neurons. This notion is substantiated by the observation that *unc-2* animals become hypercontracted after prolonged exposure to aldicarb and suggests the release of ACh from at least some motor terminals.

Several mechanisms could account for residual neurotransmitter release in *unc-2* animals. As shown in Figure 1*B*, there are two other predicted Ca channel α_1 subunits in *C. elegans*. One of these, the putative L-type channel encoded by *egl-19*, is thought to act predominantly in muscle, however it is also expressed in a subset of neurons (Lee et al., 1997), and thus could play a role in neurotransmission at some terminals. There are also two novel four domain Ca channel-like α_1 subunits encoded by *nca-1* and *nca-2* (Fig. 1*B*) (T. P. Snutch and K. Hamming, unpublished results), and a T-type-like Ca channel encoded by *cca-1* that may play a role in regulating synaptic activity, although no mutations that affect neurotransmission have been mapped to these parts of the genome. The possibility of either overlapping or redundant roles in synaptic transmission could be examined in the future by the analysis of double and triple mutants of these genes. Alternatively, it is possible that the viability of *unc-2* null mutants is due, at least in part, to the spontaneous release of ACh from the motor neurons. The presence of spontaneous miniature postsynaptic currents has been demonstrated in the absence of Ca (Richmond and Jorgensen, 1999), and it is possible that even in the absence of UNC-2 protein, sufficient ACh release occurs to maintain viability.

UNC-2 and UNC-36 likely function in the same channel complex

The *unc-36* gene encodes a polypeptide that is highly similar to the Ca channel α_2/δ subunits expressed in mammals (Lee et al., 1997). Several observations suggest that UNC-2 and UNC-36 function together *in vivo*. First, mutations in the *unc-36* gene result in movement and egg-laying defects that are similar to those exhibited by *unc-2(null)* mutants. Second, *unc-2* and *unc-36* mutants also exhibit very similar responses to the AChE inhibitor aldicarb (Nguyen et al., 1995) and also similar defects in adaptation to dopamine and serotonin (Schafer and Kenyon, 1995; Schafer et al., 1996). Third, mutations in these genes also exhibit similar genetic interactions; *unc-36; egl-19* and *unc-2; egl-19* double mutants are both essentially paralyzed and are indistinguishable in this respect (Schafer et al., 1996). Finally, *unc-36; unc-2* double mutants are indistinguishable from either single mutant in most behavioral assays, suggesting that these genes function in many of the same pathways (Schafer et al., 1996).

We also find suggestive evidence that UNC-36 activity is required for the functional expression of the UNC-2 Ca channel complex. For example, the *unc-2(ra612)* allele reduces, but does not eliminate, *unc-2* function. However, *unc-36; unc-2(ra612)* double mutant phenotype is identical to the *unc-2(null)* phenotype. Because the absence of *unc-36* ($\alpha_2\delta$ subunit) function has the same effect as the absence of *unc-2* (α_1 subunit) function, the $\alpha_2\delta$ subunit must be essential for the activity of the complex. This conclusion is consistent with results from a number of surrogate expression systems wherein co-expression of a cloned $\alpha_2\delta$ subunit is necessary for the expression of detectable whole-cell Ca currents.

The ra612 mutation alters channel biophysical properties

The *ra612* mutation alters a glycine residue that is located in the C terminal region of the protein, nine residues downstream of a Ca binding EF-hand motif and upstream of a calmodulin binding IQ motif, both implicated in regulating Ca channel function (DeLeon et al., 1995; Lee et al., 1999; DeMaria et al., 2001). All HVA Ca channels cloned to date contain a glycine residue at the homologous position, and it was of interest to determine whether the alteration in this region of the channel affected biophysical properties. Electrophysiological analysis of $\alpha_{1A}/Ca_v2.1$ channels harboring the *ra612* (G1817R) mutation showed that compared with wild-type that a stronger depolarization is required to open the mutant channels which, once open inactivated more rapidly, thereby terminating Ca influx sooner. In addition, a hyperpolarizing shift in the steady-state inactivation curve indicated a significant reduction in the number of channels available for opening at a given membrane potential.

Although we are cautious about inferring the exact *in vivo* physiological implications of these results, they are consistent with the phenotypic observations that suggest that the *ra612* mutation does not result in the complete elimination of channel function. For example, the apparent decrease in neuronal activity in *unc-2(ra612)* animals could be attributed to diminished Ca influx through the mutant channels. The increased rate of inactivation together with the changes in current–voltage properties would be predicted to reduce Ca influx resulting in decreased neurotransmitter release.

The mechanism underlying the increased rate of inactivation does not appear to be a direct alteration of Ca- or current-sensitive properties of the channel. Ion substitution experiments

illustrate that the increase in the rate of inactivation of $\alpha_{1A\text{-}ra612}$ cannot be attributed to Ca-dependent modulation previously reported for L-type or N-type calcium channels (Cox and Dunlap, 1994; Ferreira et al., 1997). Potentially, the *ra612* mutation might alter or occlude sites that interact with modulatory proteins that may or may not be Ca-activated. For example, a CaMKII–PKA consensus sequence is located near the altered glycine and phosphorylation of this site, which may serve to activate or facilitate the channel, might be inhibited by the *ra612* alteration. This is just one possible model among others that will require additional investigation to determine the underlying mechanisms responsible for the altered biophysical properties of the mutant channel.

References

Babitch J (1990) Channel hands. Nature 346:321–322.

Bargmann CI (1998) Neurobiology of the *Caenorhabditis elegans* genome. Science 282:2028–2033.

Bezprozvanny I, Scheller RH, Tsien RW (1995) Functional impact of syntaxin on gating of N-type and Q-type calcium channels. Nature 378:623–626.

Blumenthal T, Steward K (1997) RNA processing and gene structure. In: *C. elegans* II. (Riddle DL, Blumenthal T, Meyer BJ, Priess JR, eds), pp117–145. New York: Cold Spring Harbor Laboratory.

Brenner S (1974) The genetics of *Caenorhabditis elegans*. Genetics 77:71–94.

Brundage L, Avery L, Katz A, Kim UJ, Mendel JE, Sternberg PW, Simon MI (1996) Mutations in a *C. elegans* Gqalpha gene disrupt movement, egg laying, and viability. Neuron 16:999–1009.

Catterall WA (2000) Structure and regulation of voltage-gated Ca^{2+} channels. Annu Rev Cell Dev Biol 16:521–555.

Cox DH, Dunlap K (1994) Inactivation of N-type calcium current in chick sensory neurons: calcium cna voltage dependence, J Gen Physiol 104:311–336.

de Leon M, Wang Y, Jones L, Perez-Reyes E, Wei X, Soong TW, Snutch TP, Yue DT (1995) Essential Ca(2+)-binding motif for Ca(2+)-sensitive inactivation of L-type Ca2+ channels. Science 270:1502–1506.

DeMaria CD, Soong TW, Alseikhan BA, Alvania RS, Yue DT (2001) Calmodulin bifurcates the local Ca2+ signal that modulates P/Q-type Ca2+ channels. Nature 411:484–489.

De Waard M, Liu H, Walker D, Scott VE, Gurnett CA, Campbell KP (1997) Direct binding of G-protein betagamma complex to voltage-dependent calcium channels. Nature 385:446–450.

Ferreira G, Jianxun Y, Ríos E, Shirokov R (1997) Ion-dependent inactivation of barium current through L-type calcium channels. J Gen Physiol 109:449–461.

Grabner M, Wang Z, Hering S, Striessnig J, Glossmann H (1996) Transfer of 1, 4-dihydropyridine sensitivity from L-type to class A (BI) calcium channels. Neuron 16:207–218.

Heinemann SH, Terlau H, Stuhmer W, Imoto K, Numa S (1992) Calcium channel characteristics conferred on the sodium channel by single mutations. Nature 356:441–443.

Jin Y, Jorgensen E, Hartwieg E, Horvitz HR (1999) The *Caenorhabditis elegans* gene unc-25 encodes glutamic acid decarboxylase and is required for synaptic transmission but not synaptic development. J Neurosci 19:539–548.

Lee A, Wong ST, Gallagher D, Li B, Storm DR, Scheuer T, Catterall WA (1999) Ca2+/calmodulin binds to and modulates P/Q-type calcium channels. Nature 399:155–159.

Lee YN, Lobel L, Hengartner M, Horvitz HR, Avery L (1997) Mutations in the α1 subunit of an L-type voltage-activated Ca^{2+} channel cause myotonia in *Caenorhabditis elegans.* EMBO J 16:6066–6076.

Lochrie MA, Mendel JE, Sternberg PW, Simon MI (1991) Homologous and unique G protein alpha subunits in the nematode *Caenorhabditis elegans*. Cell Regul 2:135–154.

McIntire SL, Jorgensen E, Horvitz HR (1993a) Genes required for GABA function in *Caenorhabditis elegans*. Nature 364:334–337.

McIntire SL, Jorgensen E, Kaplan J, Horvitz HR (1993b) The GABAergic nervous system of *Caenorhabditis elegans*. Nature 364:337–341.

Miller KG, Alfonso A, Nguyen M, Crowell JA, Johnson CD, Rand JB (1996) A genetic selection for *Caenorhabditis elegans* synaptic transmission mutants. Proc Natl Acad Sci USA 93:12593–12598.

Miller RJ (2001) Rocking and rolling with Ca^{2+} channels. Trends Neurosci 24:445–449.

Moreno HD (1999) Molecular and functional diversity of voltage-gated calcium channels. Ann NY Acad Sci 868:102–117.

Nguyen M, Alfonso A, Johnson CD, Rand JB (1995) *Caenorhabditis elegans* mutants resistant to inhibitors of acetylcholinesterase. Genetics 140:527–535.

Nonet ML, Grundahl K, Meyer BJ, Rand JB (1993) Synaptic function is impaired but not eliminated in *C. elegans* mutants lacking synaptotagmin. Cell 73:1291–1305.

Pragnell M, De Waard M, Mori Y, Tanabe T, Snutch TP, Campbell KP (1994) Calcium channel beta-subunit binds to a conserved motif in the I-II cytoplasmic linker of the alpha 1-subunit. Nature 368:67–70.

Rand JB, Nonet ML (1997) Synaptic Transmission. In: In *C. elegans* II (Riddle DL, Blumenthal T, Meyer BJ, and Priess JR, eds.). New York: Cold Spring Harbor Laboratory.

Reiner DJ, Newton EM, Tian H, Thomas JH (1999) Diverse behavioural defects caused by mutations in *Caenorhabditis elegans* unc-43 CaM kinase II. Nature 402:199–203.

Rettig J, Sheng ZH, Kim DK, Hodson CD, Snutch TP, Catterall WA (1996) Isoform-specific interaction of the alpha1A subunits of brain Ca^{2+} channels with the presynaptic proteins syntaxin and SNAP-25. Proc Natl Acad Sci USA 93:7363–7368.

Rettig J, Heinemann C, Ashery U, Sheng ZH, Yokoyama CT, Catterall WA, Neher E (1997) Alteration of Ca^{2+} dependence of neurotransmitter release by disruption of Ca^{2+} channel/syntaxin interaction. J Neurosci 17:6647–6656.

Richmond JE, Jorgensen EM (1999) One GABA and two acetylcholine receptors function at the *C. elegans* neuromuscular junction. Nat Neurosci 2:791–797.

Rongo C, Kaplan JM (1999) CaMKII regulates the density of central glutamatergic synapses in vivo. Nature 402:195–199.

Saifee O, Wei L, Nonet ML (1998) The *Caenorhabditis elegans* unc-64 locus encodes a syntaxin that interacts genetically with synaptobrevin. Mol Biol Cell 9:1235–1252.

Schafer WR, Kenyon CJ (1995) A calcium-channel homologue required for adaptation to dopamine and serotonin in *Caenorhabditis elegans*. Nature 375:73–78.

Schafer WR, Sanchez BM, Kenyon CJ (1996) Genes affecting sensitivity to serotonin in *Caenorhabditis elegans*. Genetics 143:1219–1230.

Schuster A, Lacinova L, Klugbauer N, Ito H, Birnbaumer L, Hofmann F (1996) The IVS6 segment of the L-type calcium channel is critical for the action of dihydropyridines and phenylalkylamines. EMBO J 15:2365–2370.

Sheng ZH, Rettig J, Takahashi M, Catterall WA (1994) Identification of a syntaxin-binding site on N-type calcium channels. Neuron 13:1303–1313.

Sheng ZH, Rettig J, Cook T, Catterall WA (1996) Calcium-dependent interaction of N-type calcium channels with the synaptic core complex. Nature 379:451–454.

Starr TV, Prystay W, Snutch TP (1991) Primary structure of a calcium channel that is highly expressed in the rat cerebellum. Proc Natl Acad Sci USA 88:5621–5625.

Stea A, Soong TW, Snutch TP (1995b) Voltage-gated calcium channels. In: In Handbook of receptors and channels: ligand- and voltage-gated channels. (North RA, ed). Boca Raton, FL: CRC.

Sutton KG, McRory JE, Guthrie H, Murphy TH, Snutch TP (1999) P/Q-type calcium channels mediate the activity-dependent feedback of syntaxin-1A. Nature 401:800–804.

Tam T, Mathews E, Snutch TP, Schafer WR (2000) Voltage-gated calcium channels direct neuronal migration in *Caenorhabditis elegans*. Dev Biol 226:104–117.

Tang S, Yatani A, Bahinski A, Mori Y, Schwartz A (1993) Molecular localization of regions in the L-type calcium channel critical for dihydropyridine action. Neuron 11:1013–1021.

Thomas JH (1990) Genetic analysis of defecation in *Caenorhabditis elegans*. Genetics 124:855–872.

Troemel ER, Sagasti A, Bargmann CI (1999) Lateral signaling mediated by axon contact and calcium entry regulates asymmetric odorant receptor expression in *C. elegans*. Cell 99:387–398.

Yang J, Ellinor PT, Sather WA, Zhang JF, Tsien RW (1993) Molecular determinants of Ca^{2+} selectivity and ion permeation in L-type Ca2+ channels. Nature 366:158–161.

Zamponi GW, Bourinet E, Nelson D, Nargeot J, Snutch TP (1997) Crosstalk between G proteins and protein kinase C mediated by the calcium channel alpha1 subunit. Nature 385:442–446.

Zwaal RR, Ahringer J, van Luenen HG, Rushforth A, Anderson P, Plasterk RH (1996) G proteins are required for spatial orientation of early cell cleavages in *C. elegans* embryos. Cell 86:619–629.